Enhanced 3D Seismic Image Resolution by Applied Attributes for Improved Carbonate Reservoir Characterization in Karawang Region, North West Java

Muhammad Rizki Sudarsana, Ildrem Syafri, Andi Agus Nur, and Abdurokhim

Faculty of Geology, Padjadjaran University
Jln. Raya Bandung Sumedang Km. 21 Kabupaten Sumedang, Indonesia

Corresponding Author: muhammad18436@mail.unpad.ac.id

Abstract - The study focuses on the enhancement of 3D seismic data to improve the interpretation of carbonate growth phases within Middle Miocene limestone formations in the Karawang region, north west Java. By applying a sequential workflow of various seismic attributes, including the second derivative, phase shift, frequency filter, structural smoothing, and iterative trace Automatic Gain Control (AGC), the vertical resolution of seismic events is significantly improved, from an initial dominant frequency of 22 Hz (38 m tuning thickness) to a final effective dominant frequency of 33 Hz after all enhancements. These enhancements facilitate a clearer delineation of stratigraphy, depositional patterns, and the geometry of carbonate growth cycles. The integration of well data, including wireline logs and synthetic seismograms, with enhanced 3D seismic sections provides a comprehensive understanding of subsurface features and porosity development in the target area. The enhanced data enabled the identification of four distinct carbonate growth phases, revealing complex thickness variations and depositional architectures controlled by sea-level fluctuations. This integrated approach demonstrates the critical role of optimized seismic attribute application for detailed carbonate reservoir characterization and optimizing well placement for hydrocarbon exploration and exploitation.

Keywords: seismic enhancement, carbonate growth, attributes, vertical resolution, Karawang region

Introduction

Background

Understanding the interpretation of carbonate growth on seismic data is crucial for both exploration and exploitation of hydrocarbon targets. This process aids in determining the size, geometry, and compartmentalization of reservoirs, which are essential factors for successful hydrocarbon recovery (Khalifa, 2024; Liu and Wang, 2017; Rao and Wang, 2015). Proper interpretation allows for better prediction of reservoir behaviour, optimization of drilling locations, and improvement of overall resource management. Various techniques have been developed to enhance high-frequency components in seismic data, thereby improving vertical resolution. These techniques include seismic bandwidth extension using continuous wavelet transform (Smith *et al*., 2008) and spectral balancing techniques using structure-oriented filtering and spectral decomposition (Marfurt and Matos, 2014). Automated tracking

of chronostratigraphic events, known as horizon cube interpretation, also significantly improves horizon interpretation down to the subhorizon level. By combining advanced seismic enhancement and automated event tracking, a comprehensive workflow was proposed to aid in facies and stratigraphic interpretation, particularly in the analysis of carbonate bodies in the seismic data.

The Mid Main Carbonates (MMC) are significant reef carbonate deposits formed during a prolonged transgressive phase in The Middle Miocene (Isworo, 1999; Natasia, 2024; Ratkolo, 1994) within The North West Java Basin (NWJB) (Figure 1). Previous research on MMC facies has focused on depositional models using well and core data, particularly offshore, and investigated onshore isolated reefs influenced by sea-level eustasy. More recently, comprehensive interpretations of the entire Upper Cibulakan Formation suggest a transgressive event from The Early to Late Miocene. While these studies offer detailed geological divisions of the MMC facies
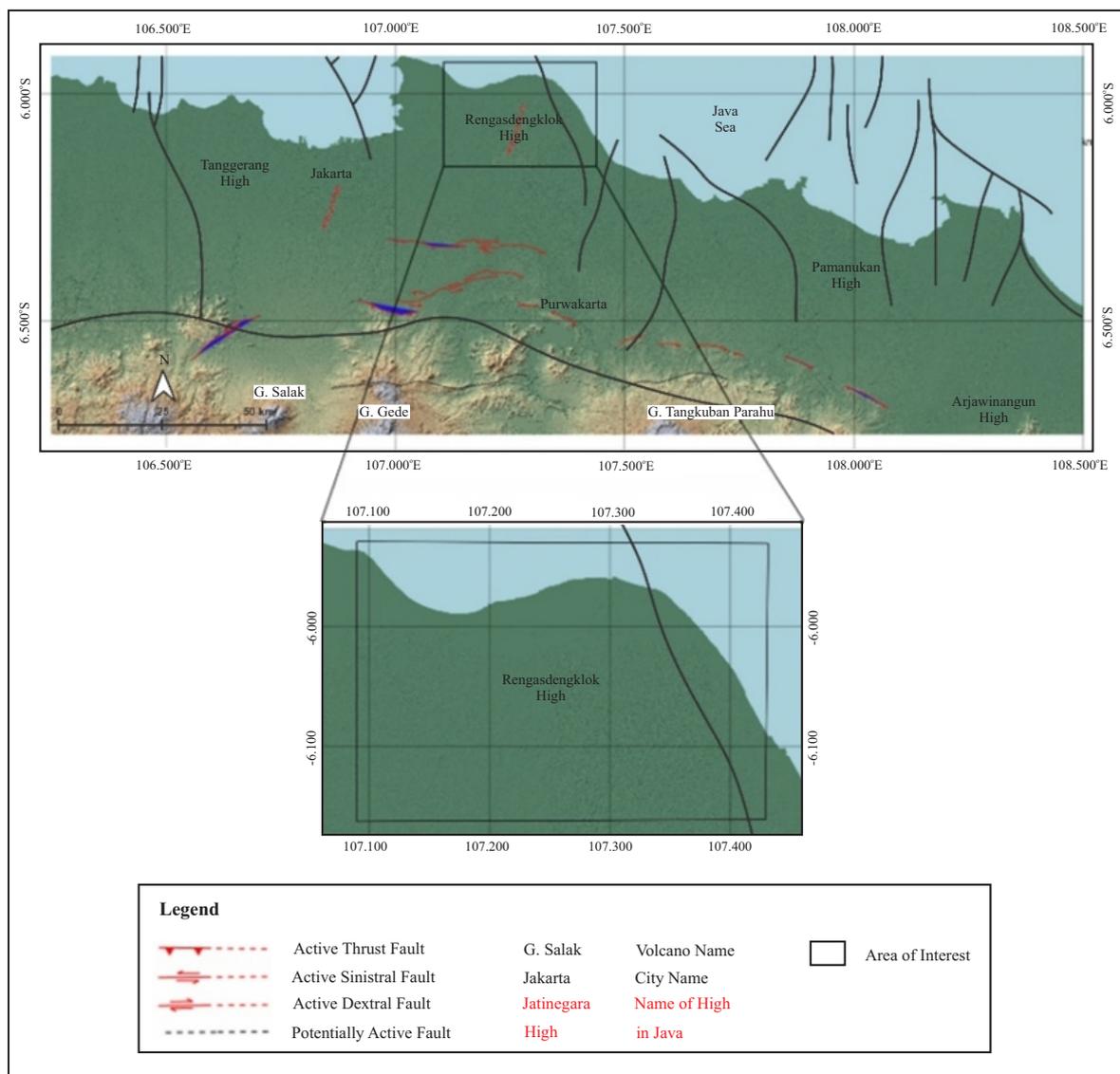

Figure 1. Digital Elevation Model illustrating surface features of the northern West Java region and the major faults developed within the studied area. The southern part of the studied area is marked by the back-arc thrust fault (Aribowo *et al*., 2022). There are four grabens (Ciputat, Kepuh, Pasir Bungur, and Cipunegara Graben) separated by the Tanggerang, Rengasdengklok, Pamanukan, and Arjawinangun basement high (Lunt, 2013). The studied area is located on the Rengasdengklok high (highlighted in black box).

402

in a petroleum context, analyses of their lateral distribution using 3D seismic data are limited. Adriansyah and McMechan (2002) conducted an intensive study on the clastic Upper Cibulakan interval using Amplitude Versus Offset (AVO) to identify thin layers, but did not interpret the MMC carbonate layers.

In this paper, the use of a systematic seismic attribute workflow was discussed to enhance data quality and vertical resolution. Information from various seismic attributes is utilized to attenuate noise and broaden the frequency bandwidth, thus improving vertical resolution. This enhanced seismic data is subsequently used for the detailed interpretation of carbonate growth cycles and their lateral distribution. By understanding this process, the proposed analysis can aid in optimizing well placement for prospect identification.

Geological and Stratigraphical Setting

The MMC in The North West Java Basin developed mainly at the paleo high areas as a result of pre-Oligocene rift tectonics (Satyana

and Purwaningsih, 2003; Sharaf *et al.*, 2005). The formation of The West Java Basin can be divided into three mains tectonic. The Eocene-Oligocene tectonic phase involved north–south oriented normal faults, forming half-graben structures with a west–east opening direction (Pubellier and Morley, 2014; Suyono *et al.*, 2005). This activity led to the formation of The Ciputat, Kepuh, Pasir Bungur, and Cipunegara Grabens, separated by The Tanggerang, Rengasdengklok, Pamanukan, and Arjawinangun Highs (Figure 1). Syn-rift sediments were deposited in these low areas. During The Late Oligocene to Late Miocene, tectonic activity shifted to compression-dominated, ceasing the rifting. The entire basin experienced post-rift events (Clements *et al.*, 2009; Clements and Hall, 2011; Pubellier and Morley, 2014; Suyono *et al.*, 2005), during which The Baturaja and Upper Cibulakan Formations were deposited (Bishop, 2000; Lunt, 2013; Satyana and Purwaningsih, 2003) (Figure 2).

The Upper Cibulakan interval ranges from Early Miocene to Late Miocene, with maximum transgression observed in The Middle Miocene,
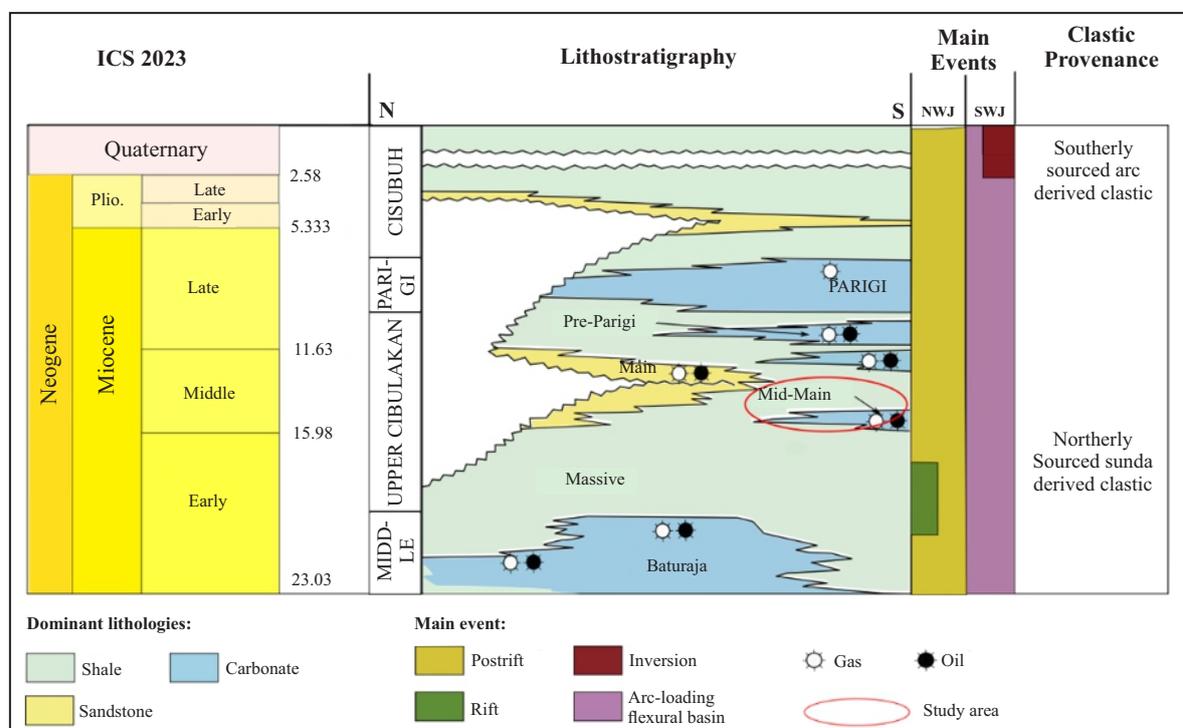

Figure 2. Miocene stratigraphic column in The North West Java Basin (modified from Natasia, 2024). Upper Cibulakan interval ranges from Early Miocene to Late Miocene. Maximum transgression is observed in The Middle Miocene, during which the Mid Main Carbonate member developed in the southern part of The North West Java Basin.

when the Mid Main Carbonate member developed in the southern part of The Northwest Java Basin. The Upper Cibulakan Formation is divided into a lower Massive member and an upper Main member. Lithostratigraphically, the Main member contains three primary intervals for hydrocarbon exploration: Main sands, MMC, and Pre-Parigi carbonate (Adriansyah and McMechan, 2002; Noble *et al*., 1991; Posamentier, 2002) (Figure 2). Main sands were deposited in a shallow marine shelf ridge environment in the northern shallower area (Posamentier, 2002), while MMC was deposited in deeper areas where clastic sediment supply was absent, favouring carbonate reef facies development (Ratkolo, 1994). Following MMC deposition, further transgressive events in the NWJB reduced clastic sediment supply from the north, intensifying carbonate deposition (Burbury, 1977; Widodo, 2018). During this period, pre-Parigi carbonates were deposited (Bukhari *et al*., 1992; Natasia, 2024). The Late Miocene to Early Pliocene saw the deposition of Parigi Formation carbonates, succeeded by The Cisubuh Formation shales (Bukhari *et al*., 1992; Burbury, 1977).

Methods and Materials

Two exploration wells (Well 1 and Well 2), equipped with wireline logs (gamma ray, neutron porosity (NPHI), density (RHOB), and sonic (DT)) and final drilling reports, were utilized for stratigraphy and depositional pattern interpretation following limestone well log interpretation standards (Moore and Wade, 2013). Lithology descriptions were obtained from side-wall core reports. The gamma ray log was employed to observe stacking patterns (constant, decreasing, and increasing upwards), and porosity logs were used to examine porosity development within each pattern. The combination of stacking patterns and porosity was crucial for delineating carbonate growth phase boundaries, leading to the identification of four distinct carbonate growth phases in the well data. Both wells were supplemented with check shot data for accurate well-to-seismic tie. Synthetic seismograms were generated by extracting seismic data sections and subsequently correlated with well data.

A 3D seismic dataset from the Karawang region, covering a 6 x 8 km² area, was used. The MMC are clearly visible on the seismic sections. One north−south, one east−west, and one southwest−northeast oriented seismic line are presented to illustrate MMC carbonate geometry (Figure 3). The initial raw seismic data had a dominant frequency of 22 Hz and an average velocity of 3,300 m/s, resulting in a tuning thickness of approximately 38 m.

The seismic data enhancement workflow comprised several steps:

1. Second Derivative Attribute: The first step involved applying the second derivative attribute to assess and improve the continuity of seismic events within the target area. This attribute sharpens seismic reflections, making them more distinct and enhancing their termination and interpolation, particularly in the internal parts of the Top MMC and Base MMC configurration. As a consequence, initially
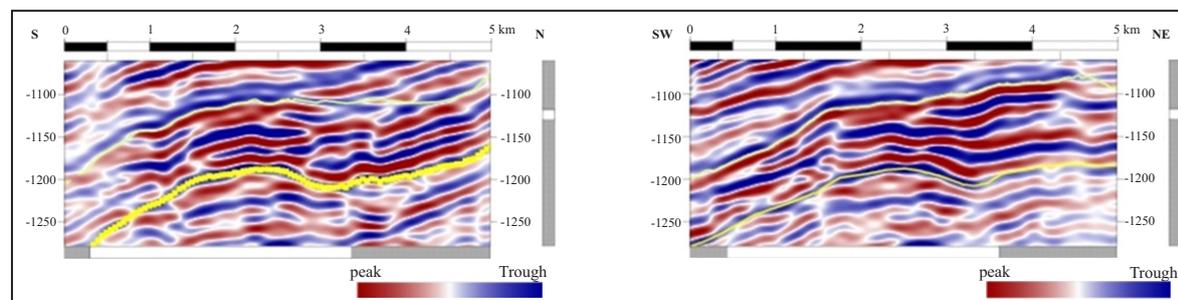

Figure 3. The left picture represents the result of seismic data quality improvement with south north direction and the right picture with southwest northeast direction. (Green horizon shows top of MMC formation).

broad seismic events (e.g. two amplitudes of peak and trough) were resolved into sharper, more separated events (*e.g.* four amplitudes) (Figure 4b).

2. Phase Shift Attribute: Due to the inherent 180 degree phase reversal caused by the second derivative attribute, a phase shift of 180 degrees was applied to restore the seismic data to its original zero-phase state (Figure 4c). This step is critical for accurate stratigraphic interpretation and well-to-seismic ties. After this step, the dominant frequency spectrum increased to 55 Hz (Figure 5).

3. Frequency Filter (Bandpass Filter): The second derivative and phase shift attributes can sometimes produce out-of-scale amplitudes (white colour in the middle of the peak and trough) due to excessively high or low amplitude values. To address this and further attenuate noise, a bandpass filter was applied (Figure 4d). The chosen parameters were: low frequency 5 Hz, low cut 8 Hz, high cut 60 Hz, and high frequency 80 Hz. These parameters were carefully selected based on spectral analysis of the raw and derivative data to remove unwanted very high or low frequencies considered noise or interference, while preserving the signal related to the MMC. This resulted in smoother, more continuous seismic data with a dominant frequency of 54 Hz (Figure 5).

4. Structural Smoothing: Structural smoothing was applied to enhance seismic event continu-
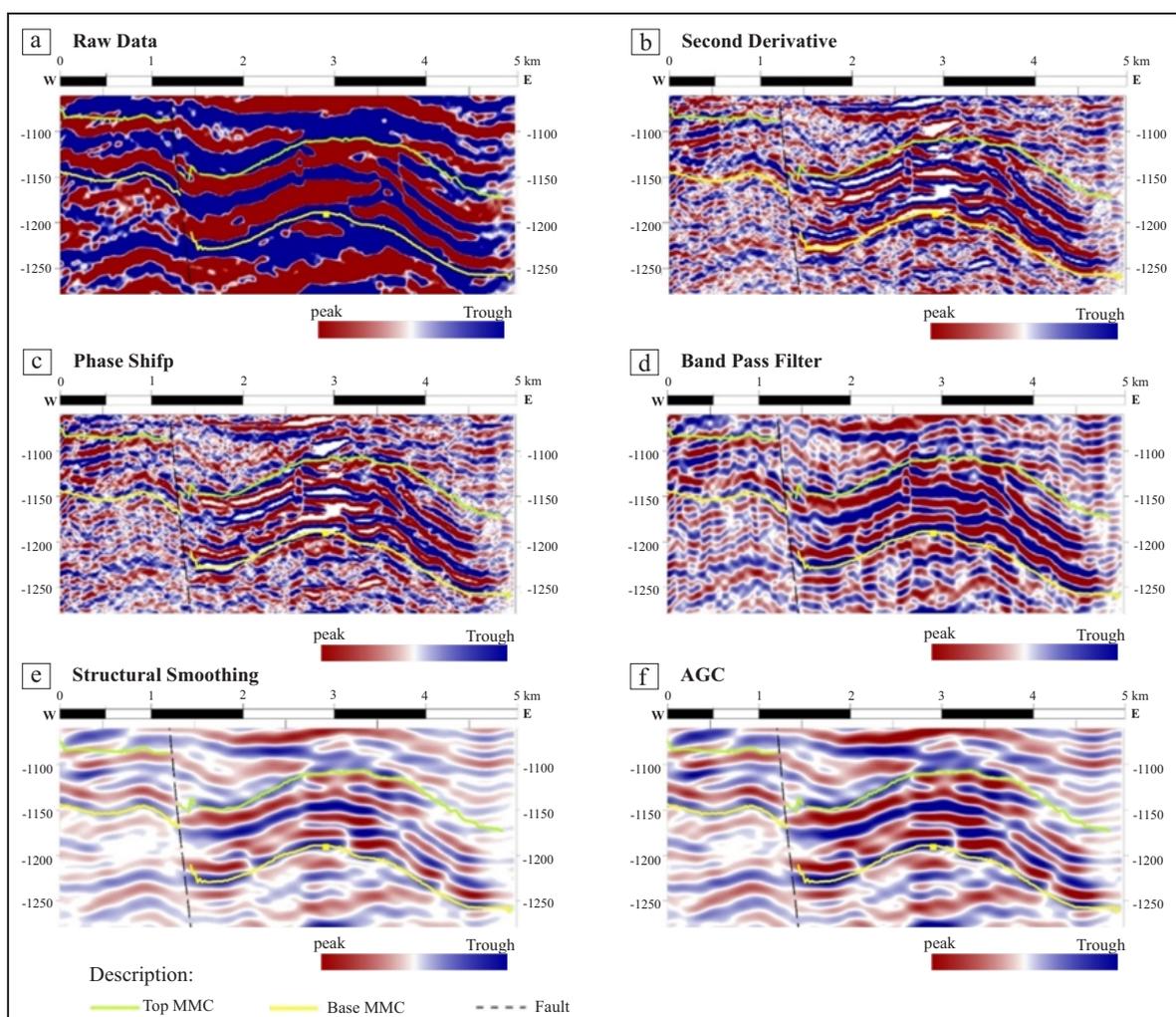

Figure 4. a) Raw data seismic, b) Attribut Second Derivative, c) Phase Shift, d) Band Pass Filter, e) Structural Smoothing, f) AGC. (Green horizon shows top of MMC formation).
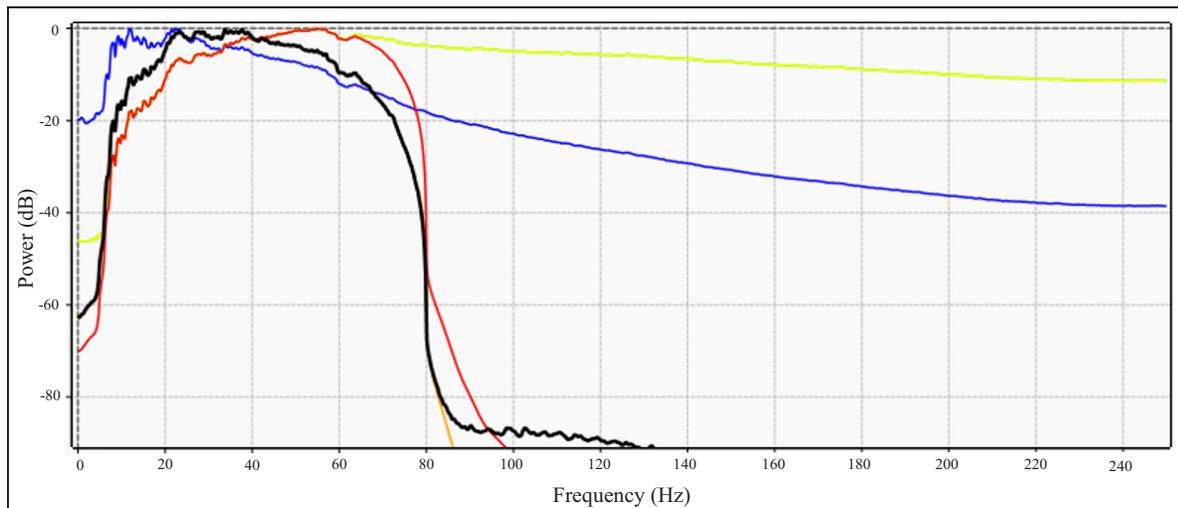
Figure 5. Frequency spectrum. The blue line represents the raw seismic data showing a peak frequency value of 12 Hz, the yellow and green lines intersecting each other are both attributes of the second derivative and phase shift with a peak frequency of 55Hz, the red line is an attribute of the band pass filter with a peak frequency of 54 Hz, and the last two lines intersecting orange and black are attributes of structural smoothing and AGC with a peak frequency of 33Hz.

ity by operating on the input signal guided by local structural dip and azimuth (Figure 4e). This attribute is particularly beneficial for improving the visualization of seismic events and aiding horizon picking, while carefully avoiding over-smoothing that could diminish subtle structural features.

5. Iterative Trace AGC (Automatic Gain Control): Finally, iterative trace AGC was utilized to balance amplitude variations across the seismic section (Figure 4f). This attribute strengthens seismic traces based on root mean square (RMS) calculations of amplitude within a specific window. The combined effect of structural smoothing and AGC contributed to overall seismic image clarity. After these final steps, the effective dominant frequency of the enhanced seismic data was 33 Hz (Figure 5), representing a significant improvement in resolution compared to the raw data's 22 Hz.

After the 3D seismic data was successfully enhanced, well-to-well correlation was conducted using the improved seismic sections. Subsequently, the geometry of each carbonate growth cycle was analyzed by observing seismic geometries and integrating them with porosity development indicated by wireline log data.

Result and analysis

Well Log Interpretation

The description of the MMC in Well 1, obtained from the well report, indicates that the limestone ranges from packstone to wackestone, with a pale yellow-brown colour and medium to hard hardness (Figure 6). On the wireline log, the MMC are characterized by a serrated gamma ray signature, generally exhibiting low gamma ray values, with a total thickness of approximately 180 m from the top depth of 1050 msTvd.

Based on gamma ray stacking patterns and porosity log characteristics, four distinct phases of carbonate growth were interpreted within the MMC interval (Figure 6):

Phase 1 (1180−1160 msTvd): The gamma ray log displays a decreasing GR upwards pattern (indicated by inverted triangles), coinciding with a decreasing porosity trend upwards.

Phase 2 (1160−1120 msTvd): The gamma ray stacking pattern shows an increasing GR trend upwards (marked by white triangles). Porosity logs indicate a relatively constant trend around 1140 msTvd, increasing towards 1120 msTvd.

Phase 3 (1120−1080 msTvd): The gamma ray stacking pattern shows a decreasing GR trend upwards, while porosity log values remain
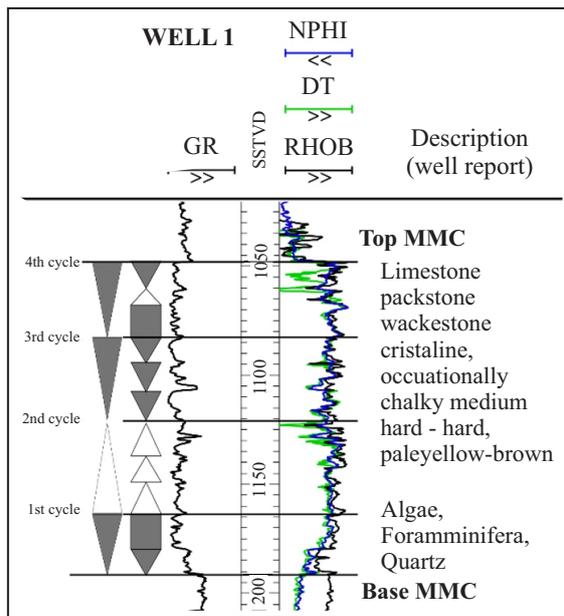
Figure 6. Mid Main Carbonate interval in Well 1. Eleven deposition patterns categorized into four carbonate growth phases can be observed based on the interpretation of gamma ray and porosity logs (white triangles and inverted gray triangles). Rock descriptions are derived from the side wall core report.

relatively constant.

Phase 4 (1080–1050 msTvd): Up to the top of MMC, the gamma ray pattern remains relatively constant. Porosity logs (neutron and density) show a constant range at the lower part and a slight increase towards the top, although the sonic log reveals significant differences in porosity compared to neutron and density logs.

Seismic Data Enhancement

The raw seismic data (Figure 4a) exhibits broad seismic events, making it challenging to separate the Top MMC and Base MMC horizon boundaries, which is problematic for accurate horizon picking. The application of the second derivative attribute significantly improved the termination and continuity of seismic events, especially in the internal parts of the MMC configuration (Figure 4b). This is evident by the visual splitting of two initial amplitudes (peak and trough) into four distinct amplitudes (Figure 4b), demonstrating a clear enhancement in vertical resolution.

A 180-degree phase shift attribute was then applied to restore the seismic data to its original

zero-phase polarity, which is crucial for correct stratigraphic interpretation and well ties (Figure 4c). The dominant frequency spectrum at this stage increased to 55 Hz (Figure 5). While the second derivative and phase shift attributes enhanced resolution, they also introduced out-of-scale amplitudes. The subsequent application of a bandpass filter effectively removed these very high or low frequencies considered noise, resulting in smoother and more continuous seismic data (Figure 4d). The dominant frequency after bandpass filtering remained high at 54 Hz (Figure 5).

Finally, structural smoothing (Figure 4e) and AGC (Figure 4f) attributes were applied. Structural smoothing improved the smoothness and continuity of seismic events guided by local structures, aiding in horizon picking. AGC served to balance amplitudes across the seismic volume. While these attributes are vital for overall data quality and interpretation, it is noted that the final effective dominant frequency after these steps reduced to 33 Hz (Figure 5). This represents a significant improvement in vertical resolution compared to the initial 22 Hz raw data. Based on the 33 Hz dominant frequency and an average velocity of 3300 m/s, the effective tuning thickness of the enhanced data is approximately 25 m, allowing for better delineation of features previously below resolution limits.

DISCUSSION

Well to Well Correlation

The enhanced seismic data has proven invaluable in facilitating inter-well correlation. In the absence of enhanced seismic support, correlating available well data would be significantly more challenging, primarily due to the inherent variability in gamma ray values and GR log patterns observed across different wells. Seismic enhancements provide a unified perspective and clarity in identifying geological features and stratigraphic markers, offering a much clearer picture of carbonate thickening and thinning in each growth phase. Well correlation, illustrated in Figure 7,
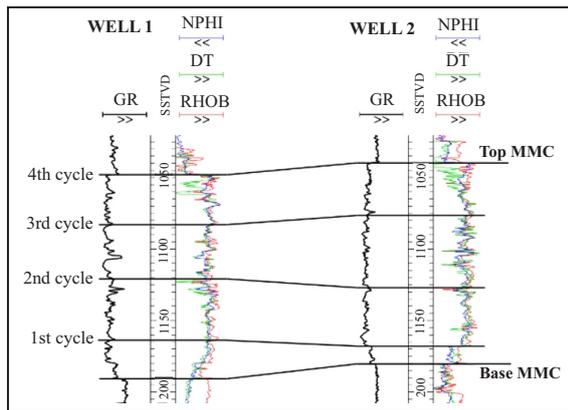
407

Figure 7. Well to well correlation illustrating variations in thickness across each carbonate growth cycle in the MMC. In the first stage, thicker carbonate development is observed in Well 2, while subsequently, the growth rates between the two wells show no significant differences.

reveals a crucial discrepancy in the first growth cycle: Well 1 exhibits a thicker carbonate development compared to Well 2, which has a thinner

thickness for this initial phase. This difference is clearly visible in the enhanced seismic section (Figure 8).

This contrasts with the initial lithostratigraphic definition where the base of the MMC is simply defined as the first carbonate facies in the wells. In contrast, the enhanced seismic horizon continuity aligns more accurately with chronostratigraphic events. The chronostratigraphic base of the MMC that matches the position in Well 1 appears to be stratigraphically lower than the base MMC in Well 2. This is further supported by the presence of onlap configurations from the area around Well 2 towards the mounded configuration in Well 1 (Figure 8) , suggesting that carbonate growth in the area around Well 1 is slightly older compared to Well 2. In subsequent growth phases (second, third, and fourth cycles), the thicknesses observed in both wells do not differ significantly.
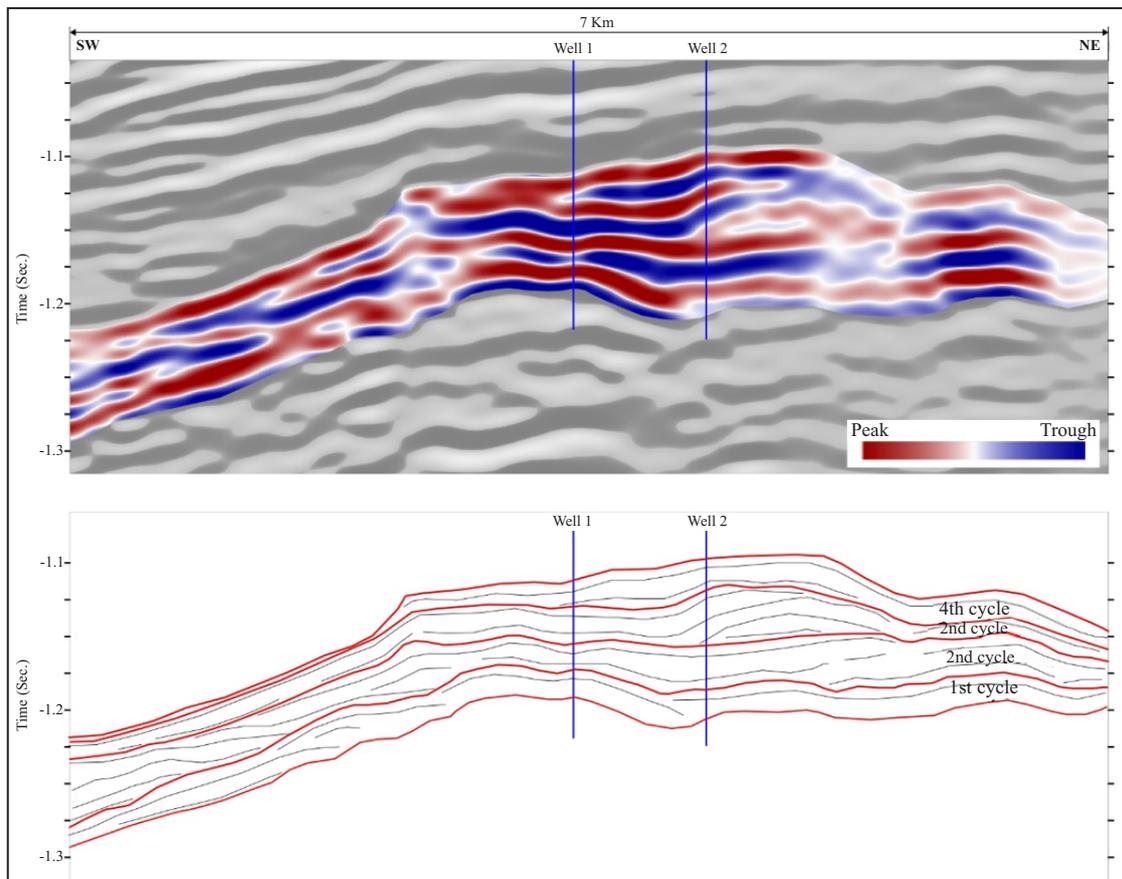

Figure 8. Southwest-northeast seismic interpretation line illustrating the growth cycles of the MMC. Note the onlap configuration from Well 2 to Well 1 area in the first cycle indicating the different starting time of carbonate development. Refer to Figure 3 for location of this line.

Carbonate Development Cycles

Detailed analysis of the enhanced seismic data, integrated with well logs, allowed for the interpretation of four distinct carbonate growth cycles:

- **First Cycle:** A northward-moving onlap configuration (retrogradation) is observed in the southern area of Well 1. Around Well 1 (central area), a relatively small mounded geometry is seen, followed by another on-lap configuration to the north. We interpret these configurations as the initial stages of MMC carbonate growth. The retrogradation in the southern area indicates that the early development of the MMC occurred during a transgressive phase, consistent with carbonate platform evolution on a shallow-marine shelf (Sirodj *et al.*, 2022; Ehrenberg *et al.*, 2024), where the sea level rise outpaced the growth of the MMC. The strong amplitude reflection in the seismic data, despite lacking well data confirmation for carbonate facies in this specific location, supports this interpretation. The mounded geometry likely represents the first vertical growth of the MMC carbonates, suggesting a stillstand period following the initial transgressive phase (Suryana *et al.*, 2023). This is supported by well data, where the gamma ray log shows an initial high value (indicative of shaly intervals) that then drops significantly (indicating cleaner carbonates). The porosity log shows a relatively constant low value at the top of the first cycle, suggesting that this part of the carbonate was likely always submerged (Jambak *et al.*, 2015; Sirodj *et al.*, 2022). This condition prevented significant porosity enhancement at the top of the first growth cycle.

- **Second Cycle:** This cycle also shows retrogradation in the southern area, transitioning into sub-parallel geometries with progradation. We interpret this as a second sea-level transgression, consistent with Middle Miocene transgressive events (Adlan *et al.*, 2025). This transgression likely began with a brief sea-level drop, causing the mounded feature from the first cycle to cease development and instead form retrogradation in the south. We speculate that this sea-level drop did not expose the first cycle carbonates above sea level, as the porosity in both wells remains relatively constant during this period. The retrogradational geometry then transitions to sub-parallel with progradation at the margins, indicating intensive carbonate growth that kept pace with the rising sea level. Notably, porosity near the top of the second cycle in Wells 1 and 2 shows a significant increased, suggesting that a sea-level drop at the end of this cycle exposed the carbonates, leading to porosity enrichment.

- **Third Cycle:** This cycle begins with a mounded geometry around Well 2 to the north, followed by sub-parallel configurations above. We interpret this as the third transgressive phase in the study area. In this cycle, the mounded geometry previously around Well 1 shifts northward towards Well 2, supporting the general landward migration of the carbonate factory during the MMC due to continued sea-level rise. This sea-level rise appears to have been matched by carbonate growth, resulting in generally sub-parallel seismic configurations with progradation at the margins (Rosid *et al.*, 2021; Adlan *et al.*, 2023). Porosity values in the third cycle in Wells 1 and 2 remain relatively constant with only slight spikes, and there is no significant porosity enrichment at the top. This suggests that this cycle did not necessarily end due to a sub-aerial exposure event via sea-level fall, but potentially due to reduced accommodation space or changes in carbonate factory productivity (Adlan and John, 2023).

- **Fourth Cycle:** The fourth carbonate growth cycle begins with another mounded geometry around Well 2, indicating continued transgression and providing accommodation space for further carbonate growth (Suryana *et al.*, 2023). This fourth cycle of carbonate growth appears to have matched the sea-level rise, resulting in laterally extensive growth. Porosity

values also show a significant increase at the top of the fourth cycle, indicating a notable porosity enrichment at the end of MMC growth. A pronounced sea-level drop at the end of the fourth cycle likely exposed these carbonates, leading to the relatively thick layer of enriched porosity observed in the well data.

CONCLUSIONS

Enhanced 3D seismic data significantly facilitated well-to-well correlation and the detailed analysis of carbonate growth cycle geometries, integrating seismic data with porosity development from wireline logs. The Mid Main Carbonates (MMC) exhibit a complex pattern of gamma ray and porosity log variations, indicating multiple phases of carbonate growth and differing porosity characteristics throughout the interval.

The seismic enhancement workflow, progressing from a raw data dominant frequency of 22 Hz to an effective dominant frequency of 33 Hz, significantly improved vertical resolution, enabling clearer event separation. This enhancement proved crucial for inter-well correlation, overcoming the challenges posed by variability in gamma ray values and GR log patterns across wells. It provided a unified and clear perspective for identifying geological features and stratigraphic markers, particularly in illustrating carbonate thickening and thinning during each growth phase. For example, Figure 8 clearly shows that Well 1 exhibits a thicker first growth cycle compared to Well 2, a difference directly observed in the enhanced seismic section. In later growth phases, the thicknesses in both wells are more similar.

Overall, the identified four carbonate growth cycles illustrate distinct stages of transgression, carbonate growth, and periods of exposure and porosity enrichment, dynamically driven by changes in sea level. This integrated approach provides a robust framework for detailed characterization of carbonate reservoirs and improves confidence in subsurface interpretation for exploration and development.

REFERENCES

Adlan, Q. and John, C. M., 2023. Clumped isotope record of individual limestone fabrics: A potential method to constrain the timing of oil migration. *Chemical Geology*, 616, 121245. DOI:10.1016/j.chemgeo.2022.121245

Adlan, Q., Kaczmarek, S. E., and John, C. M., 2023. Clumped Isotope Reordering and Kinetic Differences in Co-Hosted Calcite and Dolomite Minerals throughout Burial Diagenesis and Exhumation. *Minerals*, 13 (12), 1466.

Adlan, Q., John, C. M., Fadhillah, R. A., and Al Gharbi, W. M., 2025. Stratigraphic Controls on Middle Miocene Sequence in the Eastern North Sumatra Basin: A Forward Modeling Approach. *Marine and Petroleum Geology*. https://ssrn.com/abstract=5149310. https://doi.org/https://dx.doi.org/10.2139/ssrn.5149310

Adriansyah, A. and McMechan, G.A., 2002. Analysis and interpretation of seismic data from thin reservoirs: Northwest Java Basin, Indonesia. Geophysics, 67, p.14-26. DOI:10.1190/1.1451317.

Aribowo, S., Husson, L., Natawidjaja, D.H., Authemayou, C., Daryono, M.R., Puji, A.R., Valla, P.G., Pamumpuni, A., Wardhana, D.D., de Gelder, G., Djarwadi, D., and Lorcery, M., 2022. Active Back-Arc Thrust in North West Java, Indonesia. *Tectonics,* 41, e2021TC007120. DOI:10.1029/2021TC007120.

Bishop, M.G., 2000. *Petroleum System of The Northwest Java Province, Java and Offshore Southeast Sumatra, Indonesia*. U.S. Geological Survey Open-File Report 99-50R. Reston, Virginia: U.S. Geological Survey. DOI:10.3133/ofr9950R.

Bukhari, T., Kaldi, J.G., Yaman, F., Kakung, H.P., and Williams, D.O., 1992. *Parigi Carbonate Buildups : Northwest Java Sea* [www Document]. URL https://archives.datapages.com/data/ipa/data/038/038001/6-1_ipa0380006-1.htm (accessed 6.7.24).

Burbury, J.E., 1977. S*eismic Expression of Carbonate Build-ups, Northwest Java Basin* [www Document]. URL https://www.ipa.or.id/en/publications/seismic-expression-of-carbonate-build-ups-northwest-java-basin (accessed 6.7.24).

Clements, B., Hall, R., Smyth, H.R., and Cottam, M.A., 2009. Thrusting of a volcanic arc: a new structural model for Java. *Petroleum Geoscience,* 15, p.159-174. DOI:10.1144/1354-079309-831.

Clements, B. and Hall, R., 2011. A record of continental collision and regional sediment flux for the Cretaceous and Palaeogene core of SE Asia: implications for early Cenozoic palaeogeography. *Journal of the Geological Society,* 168, p.1187-1200. DOI:10.1144/0016-76492011-004.

Ehrenberg, S., Neilson, J., Gómez Rivas, E., Oxtoby, N., Jayachandran, I., Qi, A., and Vahrenkamp, V., 2024. Stratigraphy and diagenesis of the Thamama-b reservoir zone and its surrounding dense zones in Abu Dhabi oilfields and equivalent Oman outcrops. *Journal of Petroleum Geology*, 47 (4), p.345-459. DOI:10.1111/jpg.12871

Isworo, H., 1999. Depositional model of the MB Field Mid-Main carbonate reservoir Offshore Northwest Java Indonesia, *In*: *Proceedings of Indonesia Petroleum Association,* 27th Annual Convention 17. Presented at the Twenty Seventh Annual Convention & Exhibition, Indonesian Petroleum Association (IPA). DOI:10.29118/IPA.870.G.186.

Jambak, M. A., Syafri, I., Isnaniawardhani, V., Benyamin, B., and Rodriguez, H. 2015. Facies and diagenetic level of the upper cibulakan and parigi formation, in randegan and palimanan area. *Indonesian Journal on Geoscience*, 2 (3), p157-166. DOI:10.17014/ijog.2.3.157-166

Khalifa, A.E., (2024). Integrated geological data, 3D post-stack seismic inversion, depositional modelling and geostatistical modelling towards a better prediction of reservoir property distribution for near-field exploration: A case study from the eastern Sirt Basin, Libya. *Journal of Petroleum Science and Engineering*, 233, 111421. DOI: 10.1016/j.petrol.2023.111421.

Liu, Y. and Wang, Y., 2017. Seismic characterization of a carbonate reservoir in Tarim Basin. *Geophysics,* 82, B177-B188. DOI:10.1190/geo2016-0517.1

Lunt, P., 2013. The Sedimentary Geology of Java, Indonesia. *Indonesian Petroleum Association*. https://archives.datapages.com/data/ipa/data/073/073001/1_ipa0730001.htm ..

Marfurt, K.J. and Matos, M.C. de, 2014. Spectral Balancing Can Enhance Vertical Resolution. *AAPG Search and Discovery Article, 41357*

Moore, C.H. and Wade, W.J., 2013. Chapter 2 - The Application of the Concepts of Sequence Stratigraphy to Carbonate Rock Sequences. In: Moore, C.H., Wade, W.J. (eds.), *Developments in Sedimentology, Carbonate Reservoirs*. Elsevier, p.23-38. DOI:10.1016/B978-0-444-53831-4.00002-1

Natasia, N., 2024. *Architecture of the Early to Late Miocene Upper Cibulakan Formation, North West Java Basin, Indonesia*, Ph.D. Thesis, Sorbonne University.

Noble, R.A., Wu, C.H., and Atkinson, C.D., 1991. Petroleum generation and migration from Talang Akar coals and shales offshore N.W. Java, Indonesia. *Organic Geochemistry,* 17, p.363-374. DOI:10.1016/0146-6380(91)90100-X.

Posamentier, H.W., 2002. Ancient shelf ridges- A potentially significant component of the transgressive systems tract: Case study from offshore northwest Java. *AAPG Bulletin.* 86. DOI:10.1306/61EEDA44-173E-11D7-8645000102C1865D

Pubellier, M. and Morley, C.K., 2014. The basins of Sundaland (SE Asia): Evolution and boundary conditions. *Marine and Petroleum Geology,* 58, p.555-578. DOI: 10.1016/j.marpetgeo.2013.11.019

411

Rao, Y. and Wang, Y., 2015. Seismic signatures of carbonate caves affected by near-surface absorptions. *Journal of Geophysics and Engineering,* 12, p.1015-1023. DOI:10.1088/1742-2132/12/6/1015.

Ratkolo, T., 1994. *Reservoir characteristics and petroleum potential of the mid main carbonate, Upper Cibulakan Group, Northwest Java Basin, Indonesia,* Master's Thesis. University of Wollongong, Australia.

Rosid, M. S., Muliandi, Y., and Hafeez, A., 2021. Pore type inversion and s-wave velocity estimation for the characterization of Salawati carbonate reservoir. *Indonesian Journal on Geoscience*, 8 (1), p.131-146. DOI:10.17014/ijog.8.1.131-146

Satyana, A.H. and Purwaningsih, M.E.M., 2003. Oligo-Miocene carbonates of Java: tectonic setting and effects of volcanism. *Proceedings of Joint Convention Jakarta*, Jakarta, Indonesia, p.1-27.

Sharaf, E., Simo, J.A. (Toni), Carroll, A.R., and Shields, M., 2005. Stratigraphic evolution of Oligocene-Miocene carbonates and siliciclastics, East Java basin, Indonesia. *AAPG Bulletin.* 89, p.799-819. DOI: 10.1306/01040504054.

Sirodj, E. G., Sunardi, E., Adhiperdana, B. G., and Haryanto, I., 2022. Parigi Carbonate Reservoir for Underground Gas Storage in West Java, Indonesia. *Indonesian Journal on Geoscience*, 9 (2), p.219-228.DOI:10.17014/ijog.9.2.219-228

Smith, M., Perry, G., Stein, J., Bertrand, A., and Yu, G., 2008. Extending seismic bandwidth using the continuous wavelet transform. *First Break,* 26 (2), p.77-84. DOI: 10.3997/1365-2397.2008003.

Suryana, E., Hutasoit, L. M., Ramdhan, A. M., Nugroho, D., and Arifin, A., 2023. Pore Pressure and Compartmentalization of Carbonate Reservoirs in Northern Madura Platform-East Java Basin, Indonesia. *Indonesian Journal on Geoscience,* 10 (3), p.297-307. DOI: 10.17014/ijog.8.1.131-146

Suyono, Sahudi, K., and Prasetya, I., 2005. Exploration in West Java: play concepts in the past, present and future, efforts to maintain reserves growth*, Proceedings, Indonesian Petroleum Association, 30th Annual. Convention and Exhibition.* Presented at the Thirtieth Annual Convention, Indonesian Petroleum Association (IPA). DOI:10.29118/IPA.748.05.G.085.

Widodo, R.W., 2018. *Evolution of the Early Miocene Carbonate: Baturaja Formation in Northwest Java Basin, Indonesia. Ph.D Thesis,* Texas A&M University.